Formation control of differential-drive robots with input saturation and constraints on formation size

Ayush Agrawal, Mukunda Bharatheesha and Shishir Kolathaya

Indian Institute of Technology (IIT) Bombay, Indian Institute of Science (IISc)
ayush.agrawal.c2021@iitbombay.org, mukundab@iisc.ac.in, shishirk@iisc.ac.in

IEEE 62nd Conference on Decision and Control
December 15, 2023

Overview

Motivation

Warehouses have units (boxes) of different weights (10kg - Tonnes) and sizes depending on the product [1]. Accordingly, they employ forklifts and advanced robots like *Stretch*. *Forklift accidents* result in nearly 90 deaths and 34900 accidents per year [2]. Mobile robots like Stretch solve this issue to some extent. With a payload of 23 kg, Stretch comes at a price of $300,000 - $500,000 [3].

Motivation

We believe that we can address these issues using methods like **cooperative control** of cheaper and smaller robots. Take, for example, Turtle Bot 3 - a well-known differential-drive. It has a payload of 15 kg and costs $636 [4]. With a cooperative control strategy, a fleet of five Turtle Bots can transport goods weighing up to 75kg across a warehouse. By changing the formation size, I can accommodate boxes of different sizes over the multi-robot formation.

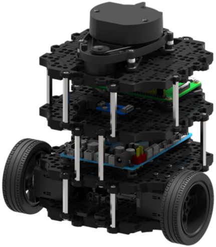

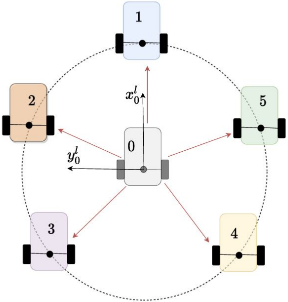

Problem Formulation

For transporting a box inside a warehouse, the following actions are required:

1. Loading the object
2. Navigation of object ✓
3. Unloading of object

For safe navigation, the formation control strategy must have the following attributes:

1. Stability of multi-robot formation during trajectory tracking (2-D) ✓
2. Obey the constraints on velocity limits ✓
3. Collision avoidance with static and dynamic objects

2-D trajectory tracking problem

Consider a robot with kinematics modelled using the following ODEs

$$\begin{aligned}\dot{x} &= \frac{R(\omega_r+\omega_l)}{2}\cos(\theta) = v\cos(\theta)\\ \dot{y} &= \frac{R(\omega_r+\omega_l)}{2}\sin(\theta) = v\sin(\theta)\\ \dot{\theta} &= \frac{R(\omega_r-\omega_l)}{L} \qquad\quad = \omega\end{aligned} \tag{1}$$

In (1), $[x, y, \theta]^T \in \mathbb{R}^3$ denotes the pose of the robot in a 2-D environment (see Fig.1). The robot has to follow a reference trajectory given by $(x_d(t), y_d(t))$ where $t \geq 0$ denotes time. Let v_{max}, ω_{max} denote the maximum permissible values of v, ω respectively.

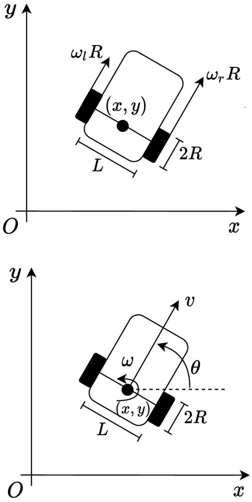

Figure: 1

Problem Formulation

We define the position errors as, $e_x(t) = x_d(t) - x(t),\ e_y(t) = y_d(t) - y(t)$. We also define the desired orientation of the robot as follows:

$$\theta_d = \arctan 2(e_y,\ e_x)\big|_{unwrap}\ \forall\ (e_x, e_y) \in \mathbb{R}^2 - (0,0) \tag{2}$$

With this definition of $\theta_d(t)$, we define the orientation error as $e_\theta(t) = \theta_d(t) - \theta(t)$. The robot will approach the reference trajectory, and stable tracking will be achieved if $e_x,\ e_y,\ e_\theta$ converge to a neighbourhood close to the origin in finite time such that

$$||e_x,\ e_y||_2 = D(t) \leq b_D, \quad |e_\theta(t)| \leq b_{e_\theta} \quad \forall\ t \geq T \tag{3}$$

for some small positive number $b_D,\ b_{e_\theta} > 0$. In other words, both $D(t),\ e_\theta(t)$ should be ultimately bounded [Theorem 4.18, 6].

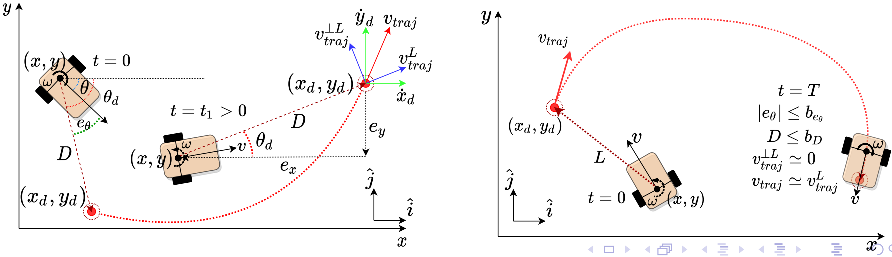

Problem Formulation: Assumptions

Assumption 1: The reference trajectory is smooth, i.e. both $x_d(t)$, $y_d(t)$ are smooth function of time, $\forall\ t > 0$. Moreover, the reference trajectory is such that it does not initiate sharp turns in the robot with respect to its current orientation, i.e.,

$$|e_\theta(t)| < \frac{\pi}{2} \tag{4}$$

Assumption 2: Define $\hat{\dot{\theta}}_d$ to be an estimate of $\dot{\theta}_d$ where,

$$\dot{\theta}_d = \frac{e_x \dot{e}_y - e_y \dot{e}_x}{D^2}, \quad D = \sqrt{e_x^2 + e_y^2} \tag{5}$$

At every time instant, we compute $\theta_d(t)$ using (2). With the value of $\theta_d(t)$ at the current and the previous time step, we can estimate $\hat{\dot{\theta}}_d$ as follows

$$\hat{\dot{\theta}}_d(t) = \frac{\theta_d(t) - \theta_d(t-\tau)}{\tau} \tag{6}$$

where $\tau \in (0,\ 1)$ represents simulation time step.

Assumption 3: The maximum translational speed of robot, v_{max} is much greater than $|v_{traj}^{sup}| = \sup_{t \geq 0} \sqrt{\dot{x}_d^2 + \dot{y}_d^2}$

Tracking controller with input saturation

Theorem

Consider a robot whose kinematics is defined as in (1) and has a maximum linear and angular speed as $v_{max}, \omega_{max} > 0$ respectively. The reference trajectory is described as $(x_d(t),\ y_d(t))$ that satisfies assumptions 1, 2, and 3. Then, stable tracking (3) is guaranteed without exceeding actuator limits if the following closed-loop negative feedback controller is applied,

$$v = v_{max} \cos(e_\theta) \frac{\eta_v D}{1 + \eta_v D} \tag{7}$$

$$\omega = (\omega_{max} - \Omega_{max}) \tanh(\eta_\omega e_\theta) + \hat{\dot{\theta}}_d \tag{8}$$

for $D = \sqrt{e_x^2 + e_y^2}$ and positive constants $\eta_v,\ \eta_\omega,\ \Omega_{max} > 0$. The choice of Ω_{max}, η_v satisfy

$$\eta_v < \frac{2(\omega_{max} - 2\epsilon_\theta)}{3 v_{max}} \tag{9}$$

$$\Omega_{max} < \omega_{max} - \epsilon_\theta \tag{10}$$

Further, $|\hat{\dot{\theta}}_d|$ is bounded $\forall\ t \geq 0$, thereby adhering to actuation limits of the robot.

Tracking controller with input saturation

1-D Problem Analogy

Consider a robot, R, chasing a point, P, in a one-dimensional space. The point, P, is moving with a constant speed v_P, and its position is denoted as $x_P(t)$. Assume that the robot, R, is located behind point P, and the initial distance between the two is large. The maximum speed of R is $v_{max} > v_P$. The speed of the robot depends on the distance, D, between R and P such that:

$$v_R = v_{max} \frac{D}{1 + D} \tag{11}$$

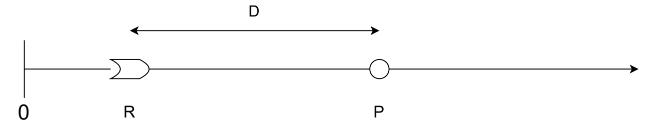

Figure: R approaching P

Tracking controller with input saturation

Solution: We can write the rate of change of D as

$$\dot{D} = v_P - v_{max}\frac{D}{1+D} \tag{12}$$

After $t = T > 0$, $\dot{D} = 0$ and the distance between the R and P will become $D^* = \frac{v_P}{v_{max}-v_P}$. Here, D^* is the equilibrium distance between R and P. Integrating (12), will give us T in terms of v_{max}, v_P and D^*. From this problem, we conclude that R will approach P in time interval $[0, T]$ such that after $t \geq T$ the distance between R and P will remain equal to D^*.

If we consider a parameter η such that

$$v_R = v_{max}\frac{\eta D}{1+\eta D} \implies D^*_\eta = \frac{v_P}{\eta(v_{max}-v_P)} \implies D^*_{\eta=5} < D^*_{\eta=1} \tag{13}$$

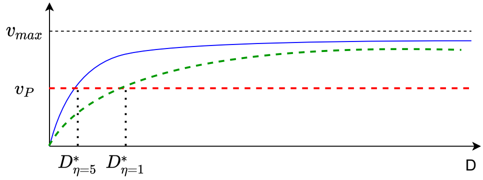

Figure: Caption

Tracking controller with input saturation

Sketch of proof (Ultimate boundedness of $D(t),\ e_\theta(t)$)

We prove the system's (1) stability under the proposed controller's (7), (8) action by proving that $D(t)$ is globally uniformly ultimate bounded, and $e_\theta(t)$ is uniformly ultimately bounded. We construct Lyapunov functions separately for $D(t)$ & $e_\theta(t)$.

For $D(t) \in \mathbb{R}_0^+,\ V_D : [0,\infty) \times \mathbb{R}^2 \to \mathbb{R}$

$$\implies V_D(D) = \frac{D^2}{2}$$

$$\implies \dot{V}_D = D\dot{D} = e_x\dot{e}_x + e_y\dot{e}_y$$

$$\dot{V}_D = \dot{x}_d e_x + \dot{y}_d e_y - \frac{\eta_v v_{max}\cos^2(e_\theta)(e_x^2+e_y^2)}{1+\eta_v D}$$

Using *Theorem 4.18* of [6], we prove $D(t)$ as globally uniformly ultimately bounded.

$$D(t) \le b_D = \frac{\sqrt{2+\zeta}}{\sqrt{2-\zeta}}(1+\zeta)\frac{|v_{traj}^{sup}|}{\eta_v\left(v_{max}\delta_\theta^2 - |v_{traj}^{sup}|\right)}$$

For $e_\theta(t) \in (-\frac{\pi}{2}, \frac{\pi}{2})$,

$$\implies V_{e_\theta}(e_\theta) = \frac{e_\theta^2}{2}$$

$$\implies \dot{V}_{e_\theta} = \dot{e}_\theta e_\theta =$$

$$e_\theta((\dot{\theta}_d - \hat{\dot{\theta}}_d) - (\omega_{max} - \Omega_{max})\tanh(\eta_\omega e_\theta))$$

Using *Theorem 4.18* of [6], we prove $e_\theta(t)$ as uniformly ultimately bounded.

$$|e_\theta(t)| \le b_{e_\theta} = \frac{\sqrt{2+\zeta}}{\sqrt{2-\zeta}}\frac{(1+\zeta)}{2\eta_\omega}\ln\left(\frac{\omega_{max}-\Omega_{max}+\epsilon_\theta}{\omega_{max}-\Omega_{max}-\epsilon_\theta}\right)$$

Here, $0 < \zeta \ll 1$ is a small positive constant. See [6, 7] for more details. We further prove in detail the boundedness of $|\hat{\dot{\theta}}_d| \le \Omega_{max}$, see [Sec. II-B, 7].

Simulation Example 1

Example 1: To illustrate the results of Theorem 1, simulations were performed in MATLAB/Simulink. We applied the proposed controller in (7), (8) to an in-built Simulink model for differential-drive kinematics. Time integration in the model was performed using the *ode*45 solver with a step size of $\tau = 0.01$s.
In this example, initial pose of the robot is $[x(0),\ y(0),\ \theta(0)]^T = [0,\ -1,\ 0.5]^T$. Simulation time is set to $T_{sim} = 200$ seconds and the robot is required to track an elliptical trajectory $[x_d(t), y_d(t)] = \left[10\cos(\frac{2\pi t}{T_{sim}}), 6\sin(\frac{2\pi t}{T_{sim}})\right]$ until the end of simulation time. Chosen control parameters are listed in Table 1.

Controller parameters			
Parameter	Value	Parameter	Value
R	$0.02m$	η_v	10
L	$0.09m$	η_ω	10
$\omega_{r,\ l}^{max}$	$52rads$	τ	0.01
v_{max}	0.52 ms	ϵ_θ	$0.1rads$
ω_{max}	$11.5rads$	Ω_{max}	$7.9rads$

Table: 1

Simulation Example 1: Results

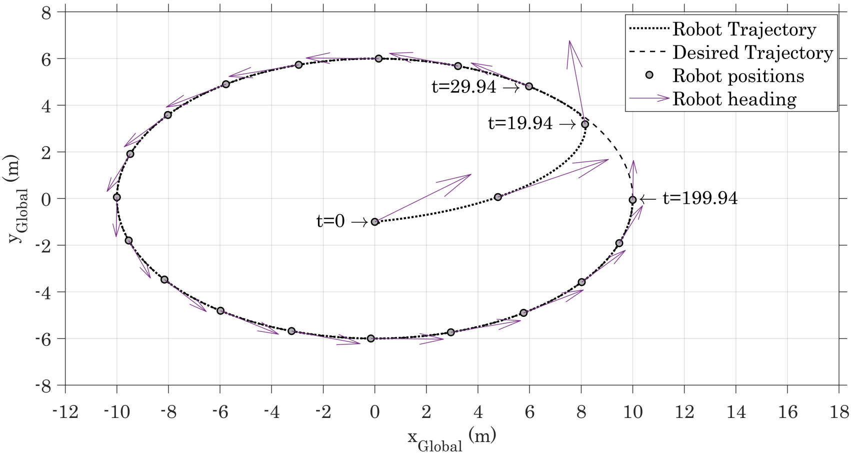

Figure: Differential drive robot tracking elliptical trajectory using proposed controller (7), (8)

Simulation Example 1: Results

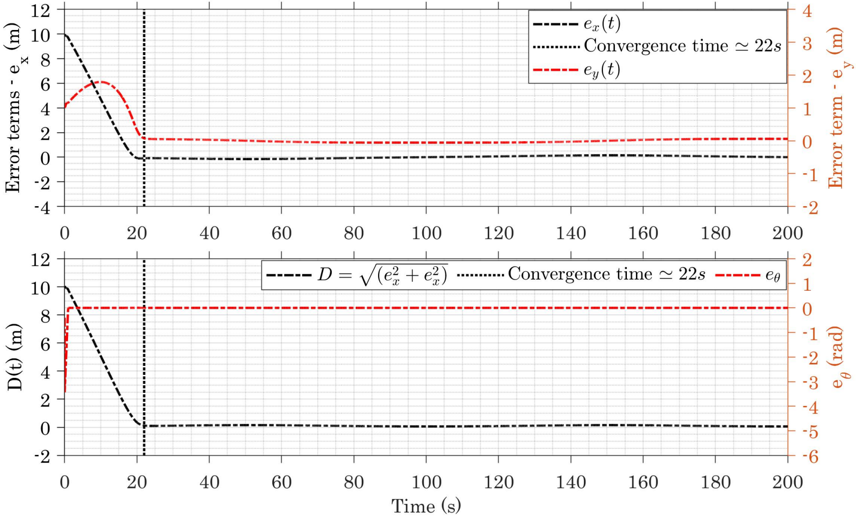

Figure: Error terms - e_x, e_y, D, e_θ converging to neighbourhood around zero.

Simulation Example 1: Results

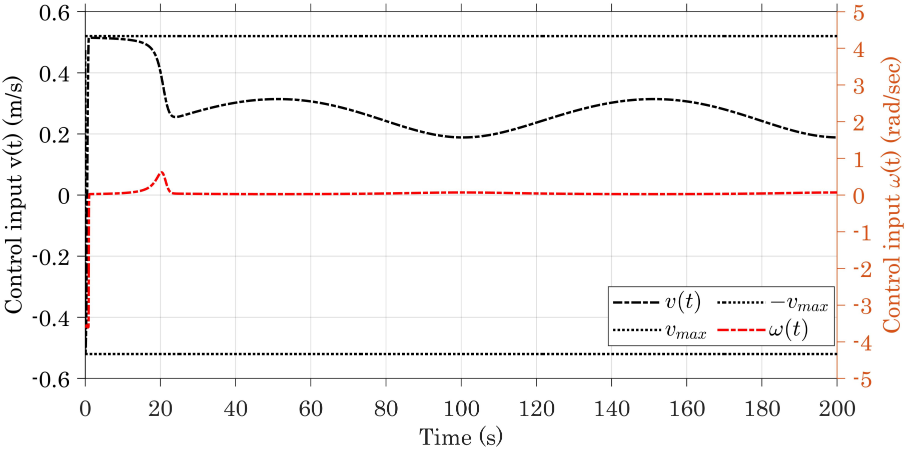

Figure: Control inputs $v(t)$, $\omega(t)$ and their saturation limits

Simulation Example 1: Results

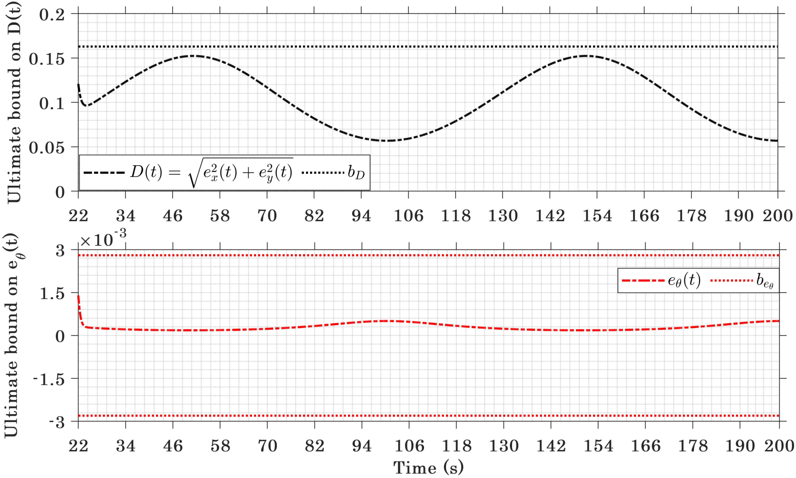

Figure: $D(t)$, $e_\theta(t)$ ultimately bounded by $b_D = 0.163m$, $b_{e_\theta} = 2.8 \times 10^{-3} rad$ respectively, for $t > 22s$

Multi-robot formation control

We solve the formation control problem using the virtual structure method. In this method, each robot subscribes to the pose information of virtual leader, $[x_0,\ y_0,\ \theta_0]$. In addition to this information, the robot also knows its local position relative to the leader. We primarily focus on circular formation. Hence, we specify the local position of robots w.r.t virtual leader using polar coordinates $(R_f,\ \alpha_i)\ \ \forall\ i \in \{1, 2, ..., N\}$. Using the above information, each robot computes its own desired trajectory. It must be noted that the formation center will coincide with the virtual leader once the formation is generated.

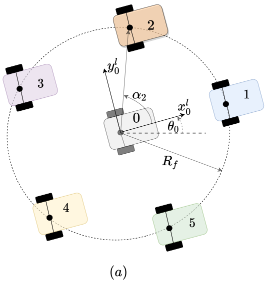

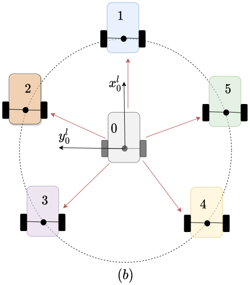

Figure: Circular formation of robots around virtual leader

Arrangement of robots in the formation

We particularly consider the circular formation and analyze the effects of its size on the kinematics of follower robots. We denote the formation radius by R_f.

At a particular instance of time, say $t \geq 0$, let $B_i^{des} = [x_i^{G.des}, y_i^{G.des}]^T$ be the desired global position of the i^{th} robot in the formation, and $b_i^{des} = [x_i^{l.des}, y_i^{l.des}]^T$ be its desired local position with respect to the coordinate system attached to the virtual leader $\forall\ i \in \{1, 2, ..., N\}$. The desired local position of the i^{th} robot (b_i^{des}) relative to the virtual leader is defined using polar coordinates, (R_f, α_i).

$$b_i^{des} = \begin{bmatrix} x_i^{l.des} \\ y_i^{l.des} \end{bmatrix} = \begin{bmatrix} R_f \cos(\alpha_i) \\ R_f \sin(\alpha_i) \end{bmatrix} \tag{14}$$

$$B_i^{des} = \begin{bmatrix} x_i^{G.des} \\ y_i^{G.des} \end{bmatrix} = \begin{bmatrix} x_0 \\ y_0 \end{bmatrix} + \begin{bmatrix} R_f \cos(\theta_0 + \alpha_i) \\ R_f \sin(\theta_0 + \alpha_i) \end{bmatrix} \tag{15}$$

Here, $[x_0, y_0, \theta_0] \in \mathbb{R}^3$ is the pose of the virtual leader.

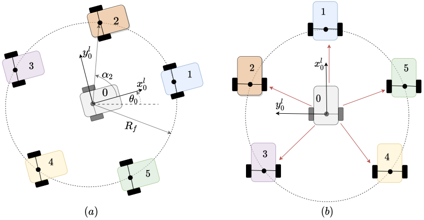

Effect of formation size on kinematics of robots

Assumption 4: The formation radius R_f is strictly less than the minimum radius of curvature of the reference trajectory $[x_d(t),\ y_d(t)]$ for the center of the formation circle, i.e.,

$$R_f < R_{des}^{min} = argmin_{t>0} \left| \frac{(\dot{y}_d^2 + \dot{x}_d^2)^{1.5}}{\dot{x}_d \ddot{y}_d - \dot{y}_d \ddot{x}_d} \right| \tag{16}$$

and the choice of R_f as per (16) must also satisfy the following condition

$$|v_{traj}^{sup}| \left(1 + \frac{R_f}{R_{des}^{min}}\right) < v_{max} \tag{17}$$

where $|v_{traj}^{sup}| = \sup_{t \geq 0} \sqrt{\dot{x}_d^2 + \dot{y}_d^2}$.

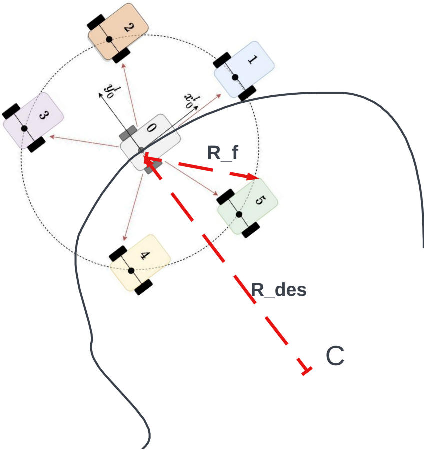

Multi-robot formation control

Theorem

Given a group of N differential drive robots. Each robot's kinematics is defined by (1). The maximum linear and angular speed of the robots are $v_{max}, \omega_{max} > 0$ respectively. Also, given a reference trajectory $[x_d(t),\ y_d(t)]$ for the formation center which satisfies assumptions 1, 2, 3. The formation radius R_f is chosen such that (16), (17) holds. Then the robots will converge to a stable formation (3) around the virtual leader if the following controller is applied $\forall\ i \in \{0, 1, 2, ..., N\}$

$$v_i = v_{max} \cos(e_{\theta_i}) \frac{\eta_v D_i}{1 + \eta_v D_i} \tag{18}$$

$$\omega_i = (\omega_{max} - \Omega_{max}) \tanh(\eta_\omega e_{\theta_i}) + \hat{\dot{\theta}}_{d_i} \tag{19}$$

for $D_i = \sqrt{e_{x_i}^2 + e_{y_i}^2}$ and positive constants η_v, η_ω, $\Omega_{max} > 0$. The choice of η_v and Ω_{max} must satisfy (9), (10).

Simulation Example 2 - A pentagonal formation

We implemented the proposed controller in (18), (19) to a group of $N = 5$ differential drive robots in Simulink. The virtual leader is modelled using (1) in Simulink. The robots have to converge to a regular pentagon-like formation circumscribed by a circle of radius $R_f = 2m$ with the virtual leader at its center. By assumption 4, we choose $R_{min}^{des} = 10m$ and $|v_{traj}^{sup}| = \frac{\pi}{10} ms$. The rest of the control parameters are the same as given in Table 1. Based on the chosen values, the virtual leader is assigned a reference trajectory given by $[x_d(t), y_d(t)] = [10\cos(2\pi t T_{sim}), 10\sin(2\pi t T_{sim})]$, where $T_{sim} = 200s$. The initial pose of virtual leader $[x_0^0, \ y_0^0, \ \theta_0^0] = [x_d(0), \ y_d(0), 1.57]$. The robots' initial poses and local angular positions (α_i) are given below.

$$\begin{bmatrix} x_1^0 & x_2^0 & x_3^0 & x_4^0 & x_5^0 \\ y_1^0 & y_2^0 & y_3^0 & y_4^0 & y_5^0 \\ \theta_1^0 & \theta_2^0 & \theta_3^0 & \theta_4^0 & \theta_5^0 \\ \alpha_1 & \alpha_2 & \alpha_3 & \alpha_4 & \alpha_5 \end{bmatrix} = \begin{bmatrix} 2 & 2 & 0 & 0 & 4 \\ 0 & 2 & 4 & -4 & 0 \\ 1 & -0.5 & 0 & -1 & 0 \\ 0 & \frac{2\pi}{5} & \frac{4\pi}{5} & \frac{6\pi}{5} & \frac{8\pi}{5} \end{bmatrix}$$

Simulation Example 2 - Pentagonal formation

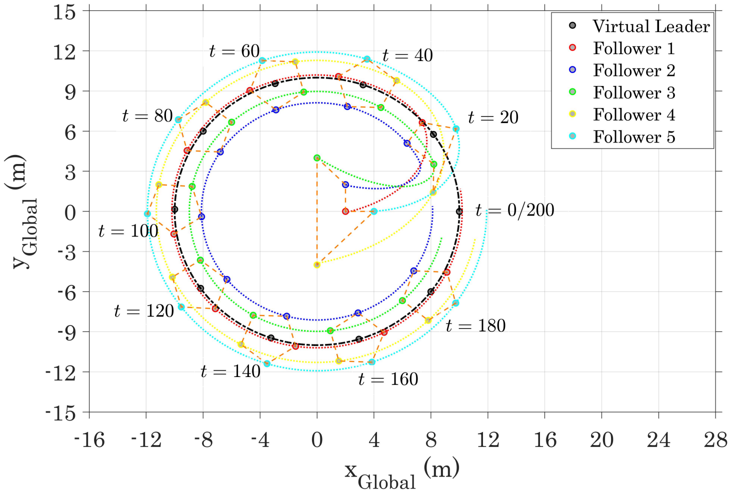

Figure: Regular pentagonal formation ($R_f = 2$) of five differential-drive robots around the virtual leader

Simulation Example 3 - $R_f > R_{des}^{min}$

Violating Assumption 4

In this example, we consider a circular formation of $N = 4$ robots with $R_f = 4m$. The reference trajectory assigned to virtual leader is $[x_d(t),\ y_d(t)] = [10\cos(\frac{2\pi t}{T_{sim}}),\ 5\sin(\frac{2\pi t}{T_{sim}})]$, where $T_{sim} = 360s$. For the chosen reference trajectory, the value of $R_{des}^{min} = 2.5m$, $|v_{traj}^{sup}| = \frac{\pi}{18}\frac{m}{s}$. Except $|v_{traj}^{sup}|$, control parameters listed in Table 1 are used. The initial pose of virtual leader $[x_0^0,\ y_0^0,\ \theta_0^0] = [x_d(0),\ y_d(0), 1.57]$. The local angular position (α_i) and initial pose of follower robots for this example are as follows

$$\begin{bmatrix} x_1^0 & x_2^0 & x_3^0 & x_4^0 \\ y_1^0 & y_2^0 & y_3^0 & y_4^0 \\ \theta_1^0 & \theta_2^0 & \theta_3^0 & \theta_4^0 \\ \alpha_1 & \alpha_2 & \alpha_3 & \alpha_4 \end{bmatrix} = \begin{bmatrix} 1 & 1 & 1 & 0 \\ 0 & 1 & -1 & -0.5 \\ 1 & -1 & 0 & -1 \\ 0 & \frac{\pi}{2} & \pi & \frac{3\pi}{2} \end{bmatrix}$$

Simulation Example 3 - $R_f > R_{des}^{min}$

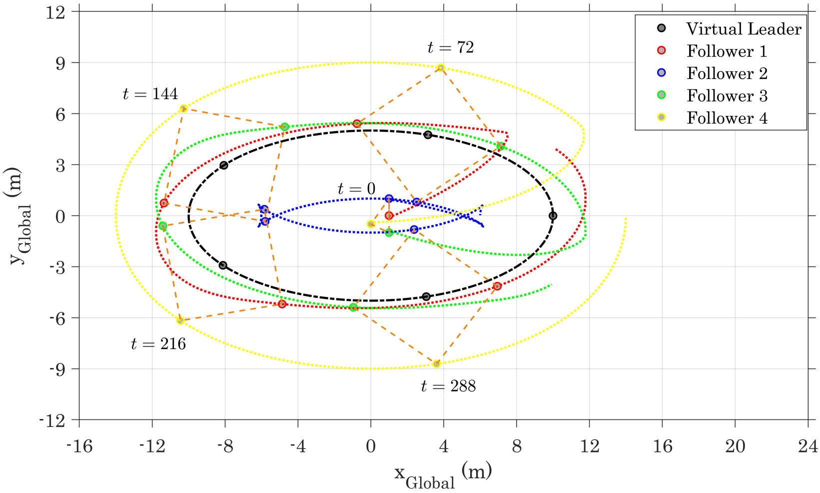

Figure: Square formation ($R_f = 4m$) of four differential drive robots around the virtual leader

Simulation Example 3 - $R_f > R_{des}^{min}$

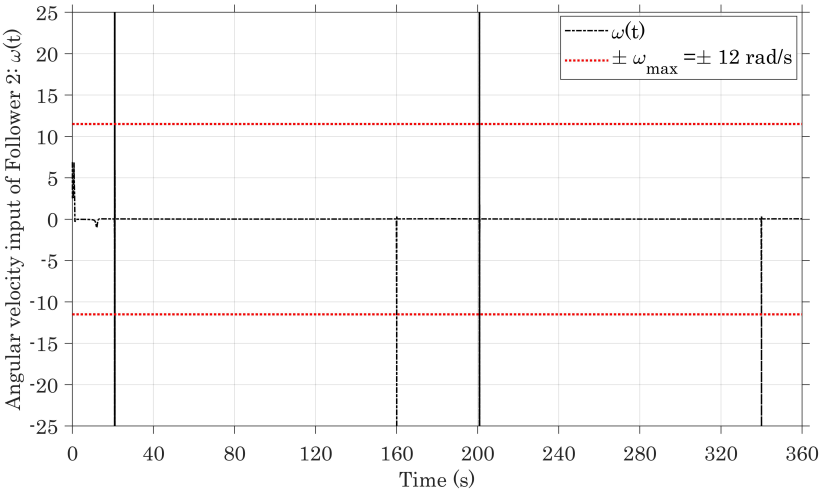

Figure: Choice of $R_f = 4m > R_{min}^{des} = 2.5m$, violated assumption 4 resulting in $\omega(t) > \omega_{max}$ in Follower 2

Future work

Having proposed a novel control law for trajectory tracking of multi-robot formation, we aim to go further by

1. Achieving similar performance under measurement noise, model uncertainties, and other actuation limitations
2. Integrating control barrier functions (CBFs) to avoid collisions with static and dynamic objects in the environment
3. Using a distributed approach to inter-robot communication to enable fault tolerance, scalability, and reliability.

Acknowledgement

The authors would like to thank the Science and Engineering Research Board (SERB) and Tata Consultancy Services (TCS) Research for the financial support provided to this research.

References

[1] Types of loads in a warehouse and their storage, Link

[2] Shocking Warehouse Safety Statistics, Link

[3] Boston Dynamics will deliver a fleet of Stretch robots to DHL, Link

[4] Turtle Bot 3, Link

[5] K. Majd, M. Razeghi-Jahromi and A. Homaifar, "A stable analytical solution method for car-like robot trajectory tracking and optimization," in IEEE/CAA Journal of Automatica Sinica, vol. 7, no. 1, pp. 39-47, January 2020.

[6] Hassan K. Khalil, 2002, *Nonlinear Systems*, Prentice Hall, 3*rd* ed.

[7] Agrawal, Ayush; Bharatheesha, Mukunda; Kolathaya, Shishir (2023): Formation control of differential-drive robots with input saturation and constraints on formation size. TechRxiv. Preprint. https://doi.org/10.36227/techrxiv.21984998

Thank you for your attention!